Entropy production and attractors: Measures to quantify uncertainty and complexity introduced by convection

Jan Niederau[1], Nele Börsing[2], Florian Wellmann[3], Christoph Clauser[1]

[1] Institute for Applied Geophysics and Geothermal Energy, E.ON Energy Research Center, RWTH Aachen University, Germany

[2] Exploration and Environmental Geophysics, Institute of Geophysics, ETH Zurich, Switzerland

[3] Numerical Reservoir Engineering, Graduate School AICES, RWTH Aachen University, Germany

jniederau@eonerc.rwth-aachen.de

Keywords: free convection, entropy production, numerical modelling, Perth Basin, Australia.

ABSTRACT

We present two measures which help quantifying the impact of oscillating, convection cells on model convergence, and model certainty:

(i) The measure of an attractor in a phase space of specific enthalpy vs change in specific enthalpy is used in order to evaluate if our model reaches a dynamic steady state after a number of time steps. Attractors are calculated first for an aquifer with homogeneous permeability and then for a case where permeability is affected by compaction. Both model solutions converge towards a point in phase space, a point attractor, thus suggesting that a dynamic steady-state is reached from the same initial conditions. The analysis indicated that the compaction scenario requires more time steps to reach this dynamic steady-state.

(ii) The thermodynamic measure of entropy production, which characterises the convective state of a system. We calculate entropy production for different scenarios of a reservoir model, where free convection occurs. Resulting entropy production values suggest that the modelled convective pattern is not significantly influenced by spatially heterogeneous permeability, but more by the reservoir structure, i.e. the effective thickness of the layer in which convection occurs. A significantly higher average entropy production of a scenario considering compaction compared to a homogeneous permeability distribution supports these findings.

1. INTRODUCTION

With a sufficient high permeability, heat transport in geothermal reservoir is usually characterised by advection. An advective heat transport by free convection occurs, when the Rayleigh number of the reservoir system exceeds a critical value. If free convection is the dominating heat transport process, the entire system can become highly non-linear. Consequently, temperature predictions at depth are increasingly uncertain in a system affected by free hydrothermal convection. In this work, we assess two measures to assess uncertainty introduced by free convection in terms of; (1) model convergence, if the model is in a representative steady state, (2) how certain the simulated convective pattern in our models is. As a study case, we study model results from the Perth Metropolitan Area (PMA), a part of the sedimentary Perth Basin in Australia, where previous work suggested the occurrence of free convection (Corbel et al., 2012; Reid et al., 2012; Sheldon et al., 2012; Schilling et al., 2013; Niederau et al., 2015).

2. METHODS

The following section explains the measures used in this study: attractors, and entropy production.

2.1 (Strange) attractors

Each state in a physical system can be fully represented by its position in an appropriate phase space. The dimension of this phase space relates to the number of variables needed to fully describe the physical system.

For example the motion of a simple swinging pendulum may be described by its angle θ [rad] and its angular velocity $\frac{\partial\theta}{\partial t}$ [rad/s] in a 2-dimensional phase space (Enns & McGuire, 2001):

$$\frac{\partial^2\theta}{\partial t^2} = -\frac{g}{l}\sin(\theta) - \beta\frac{\partial\theta}{\partial t} \qquad [1]$$

where g is gravitational acceleration in m s^{-2}, l the length of the pendulum in m, and β a damping factor. This equation describes the acceleration of the pendulum being equal to the sine of the current angle minus its damped velocity.

Figure 1 a) shows the damping of a swinging pendulum in an angle-time presentation, with the amplitude decreasing over time. The lower figure shows the same process in a phase plane. At each time interval (dots), the state of the system converges in a

spiraling orbit to the origin (0,0) where angle and angular velocity are zero, regardless of the systems initial condition.

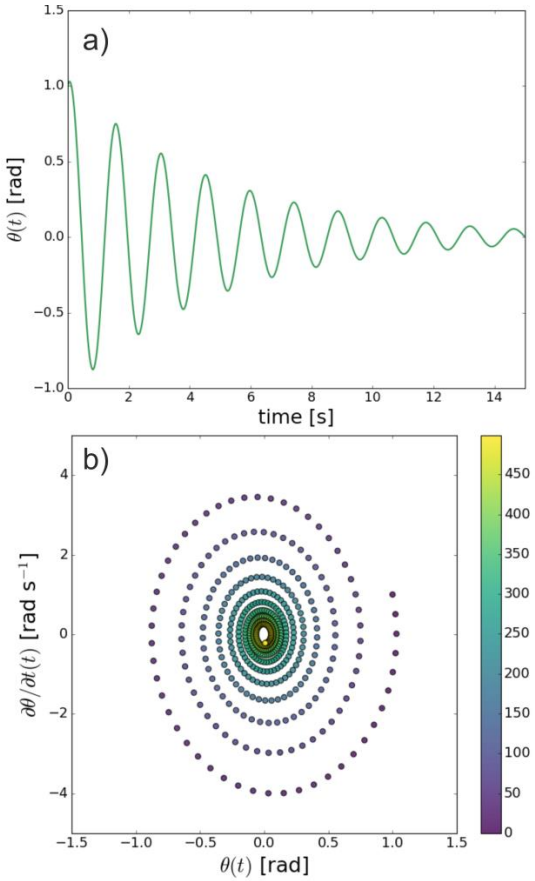

Figure 1: a) time plot of a damped, swinging pendulum showing the decreasing angle with time; b) phase space plot (colored by time-steps) showing how the pendulum converges to its equilibrium state at $\theta = 0$, $\partial\theta/\partial t = 0$, i.e.: the resting state of the pendulum.

While this example is rather trivial, it nicely displays the additional information contained in a phase space plot. In case of an undamped pendulum, an angle-time plot would show a continuous harmonic oscillation, which translates to a stable orbit around a point in phase space. Those orbited points / areas / volumes (dependent on the dimension of the phase space) are centers of attraction, or called attractors. In case of a pendulum (damped or undamped) the attractor is at the position (0,0). For non-complex systems, this is straight forward. However, attractors can also exist in time series (i.e. changes of a parameter with time) and systems, which exhibit chaotic behavior. Chaotic behavior means that the system-evolution is highly sensitive to its initial conditions (Taylor, 2010), and may not show convergent behavior on first inspection. In that case, an inspection of the phase space can be used to check if an attractor exists, which is orbited by different solutions of a chaotic system

We use a phase space representation of system variables to determine if our modelled transient, oscillating reservoir system orbits around a specific interval, i.e. an attractor. The variables (and their change in time) assessed are: fluid velocity (v) / acceleration ($\partial v/\partial t$), and Enthalpy (H) / change in Enthalpy ($\partial H/\partial t$), averaged over the whole reservoir system. Enthalpy is calculated from temperature (T) and pressure (p), using the IAPWS 97 formulation (Wagner et al., 2000). As the modelled reservoir system does not have a steady state solution due to moving convection cells, the assessment of a possible attractor orbited by the system yields a *convergence interval*. This interval, i.e. stable orbits in phase space, then encloses a dynamic steady state.

2.2 Entropy Production

The statement by Clausius in 1850: *'heat cannot pass of its own accord from a colder to a hotter body'* (Kern and Weisbrod, 1967) lays the foundation for the classical definition of entropy production. Entropy (S) is an extensive quantity, thus a function of the spatial extent of the system.

Consider an isolated system containing two bodies (B_1 and B_2) at different temperatures T_1 and T_2 ($T_1 < T_2$) (Fig. 2). Entropy in this system changes as heat is conducted from B_2 to B_1 in a dissipative process. During the evolution of the system towards a state of thermodynamic equilibrium is ($T_1 = T_2$), B_1 and B_2 both experience a change in Entropy (dS) in [J K^{-1}] (Wellmann, 2013).

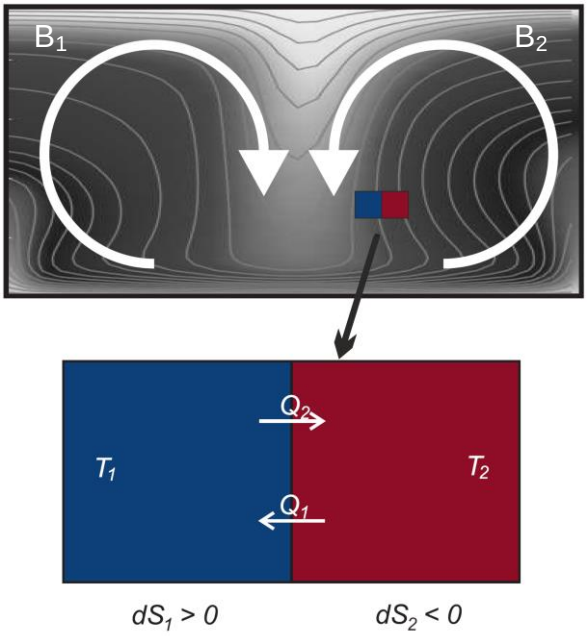

Figure 2: Schematic sketch of an isolated system, containing two bodies B_1 and B_2 with different temperatures ($T_1 < T_2$). Heat transferred from B_2 to B_1 yields an irreversible production of entropy $dS_1 > 0$ (modified from Wellmann, 2013, Börsing, 2015).

$$dS_1 = \frac{dQ_1}{T_1} \; and \; dS_2 = \frac{dQ_2}{T_2} \qquad [2]$$

The total change in Entropy would then be

$$dS = dS_1 + dS_2 \quad [3]$$

In isolated systems, the first law of thermodynamics states: $dQ_1 = -dQ_2$, thus equation [3] reduces to

$$dS = dQ_1 \left(\frac{1}{T_1} - \frac{1}{T_2}\right) \quad [4]$$

As long as $T_1 < T_2$, dQ_1 is positive. Thus, the global change in Entropy (dS), the Entropy production, can only increase and approaches zero as the difference between T_1 and T_2 decreases.

Looking at a geothermal reservoir system, these equations need to be extended. Bejan (2013) extends a definition for entropy production by Tolman and Fine (1948) to describe Entropy production in a porous medium as

$$\frac{dS}{dt} = -\frac{q''}{T^2} \cdot \nabla T + \frac{\mu_f}{T} \phi_v \geq 0 \quad [5]$$

with q''being a vector describing the transient specific heat flow in [W m^{-2} s^{-1}], μ_f the dynamic viscosity of the fluid in [Pa s], and ϕ_v is the viscous dissipation function. Substituting Fourier's law of heat conduction $q'' = -\lambda_m \nabla T$ in equation [5] gives

$$\frac{dS}{dt} = \frac{\lambda_m}{T^2} (\nabla T)^2 + \frac{\mu_f}{T} \phi_v \geq 0 \quad [5]$$

Equation [5] shows that two processes participate to the entropy production in a porous medium; conductive heat transfer (thermal dissipation), and internal friction (viscous dissipation) of the fluid. The latter friction part can usually be neglected for a porous medium (Nield and Bejan, 1999; Costa, 2006). Thus equation [5] can be simplified to

$$\frac{dS}{dt} = \frac{\lambda_m}{T^2} (\nabla T)^2 \geq 0 \quad [5]$$

That means, only thermal dissipation by conductive heat transfer contributes to the entropy production in a porous medium.

The schematic sketch in Figure 2 can be seen as a simplified analogue to neighbored zones of up-flow and down-flow in a convective system. Convection introduces lateral temperature gradients, which in turn cause lateral heat flow and the production of entropy. We use entropy production as a scalar measure to; a) quantify complexity / uncertainty of the geothermal reservoir system introduced by free convection, and b) to determine if heterogeneity in porosity and permeability in the reservoir is expressed by a change in entropy production.

3. GEOTHERMAL RESERVOIR SYSTEM

We apply the methods described previously on the Perth Basin, a north-south-trending sedimentary rift basin, extending about 1300 km along the south-western continental margin of Western Australia. It gradually passes into the continental shelf to the west and is bounded by the Darling Fault to the east. The major Darling Fault displaces the sedimentary fill of the Perth Basin against the Proterozoic Yilgarn Craton. Our assessment of the Perth Basin as a geothermal reservoir system focuses on its central part, including the Perth Metropolitan Area (Fig. 3).

Increased exploration for hydrocarbon resources led to extensive geological studies of the Perth Basin (see e.g. Playford et al., 1976; Cadman et al., 1994; Crostella & Backhouse, 2000). Its sedimentary fill (Permian to Cenozoic) is locally up to 15 km thick. Major aquifer units with high average porosity and permeability are suitable geothermal reservoirs (Niederau, 2014).

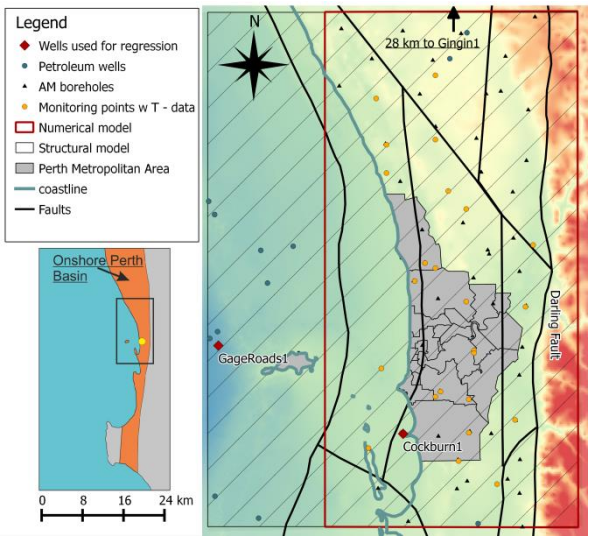

Figure 3: Map of the model area, colour coded by topography. Faults are indicated as black lines. For calculating attractors, we use the simulation results stored by monitoring points (yellow circles). For the analysis of entropy production, we use final simulation results of the entire model (red boundary)

One major potential reservoir is the Jurassic Yarragadee Aquifer, consisting mainly of fluviatile sediments, extensively assessed for its geothermal potential by the Western Australian Geothermal Centre of Excellence (WAGCoE) (Reid et al., 2012; Timms et al., 2012; DellePiane et al., 2013).

Hydrothermal conditions within the deeper Yarragadee Aquifer are highly uncertain (Pujol et al., 2015). This uncertainty is likely increased by free convection, whose occurrence in the Yarragadee is suggested by numerical simulations (Corbel et al., 2012; Reid et al., 2012; Sheldon et al., 2012; Schilling et al., 2013; Niederau et al., 2015). On the one hand, free convection generates favourable conditions for drilling geothermal wells, on the other hand, it increases the uncertainty of estimated temperatures at depth, as the position of convection cells in time is unknown.

Carried out hydrothermal simulations further suggest that the convection cells are moving with time (Schilling et al., 2013; Niederau et al., 2015). This

poses the question if, and when, the model reaches a steady state, relative to its numerical initial- and boundary conditions. Schilling et al. (2013) evaluate the change of temperature with time of some monitoring points for assessing that a dynamic steady state is reached after around 1 million years.

Simulations described in Niederau et al. (2015) show similar behaviour of oscillating convection cells. Here, simulations were run for 3 Million years, assuming a dynamic steady state is reached. In order to validate this assumption based on temperature histories at monitoring points, we assess the simulation results by plotting the model in a phase space spanned by Enthalpy of the model and its change in time.

Further, Niederau et al. (2015) assessed three different scenarios, concerning the porosity and permeability of the Yarragadee Aquifer: (1) a homogeneous porosity and permeability; (2) porosity and permeability decreasing with depth, i.e. representing compaction; (3) spatially heterogeneous porosity and permeability. We evaluate the three different scenarios for their entropy production for stating if, and how, spatially changing permeability fields affect entropy production.

4. DATA

For calculating attractors of the model, we used time dependent data from 45 monitoring points distributed in the Yarragadee Aquifer. At those monitoring points, system variables like temperature and pressure are stored at each time step over the entire simulation time of 2 Million years.

Entropy production is calculated from HDF5 files containing simulation results after 3 Million years in 3D. We calculate entropy production over all modelled geological units in 3D model space, and not only for the Yarragadee Aquifer.

5. RESULTS AND DISCUSSION

In the following, results of the phase space analysis and the entropy production will be presented.

5.1 Phase space analysis

Figure 4 shows the change of temperature with time at three exemplary monitoring points in the numerical model. The upper plot represents a scenario with homogeneous permeabilities in the Yarragadee Aquifer (scenario 1), whereas the lower plot is from a compaction scenario (scenario 2). Both plots show an oscillation in temperature over time. The presented monitoring points in the homogeneous scenario show irregular oscillation over the entire simulation period. In the compaction scenario, a relatively stable oscillation is reached after about 0.5 Ma. Before that, the onset of convection yields strong oscillation also in this scenario. Looking at temperature change with time for the compaction scenario, a dynamic steady state may be assumed after around 0.5 Ma.

However, strong oscillation is not observed at all monitoring points. Especially in the northern part of the model, where cold water infiltrates the Yarragadee Aquifer from above, almost no oscillation is observed in the models (e.g. MP 17 and MP 36 in figure 4). These observations, together with 3D visualisations of the temperature field at different times, suggest that parts of the model are in a dynamic steady state, while others are not.

For assessing if a dynamic steady state can be representatively assumed for the whole model after the simulation time of 2 Ma, we define a phase space of specific enthalpy and its change in time [H, $(\partial H/\partial t)$]. Average enthalpies of the 45 monitoring points and the time-dependent change of enthalpy are plotted within this phase space for the different scenarios (Fig. 5).

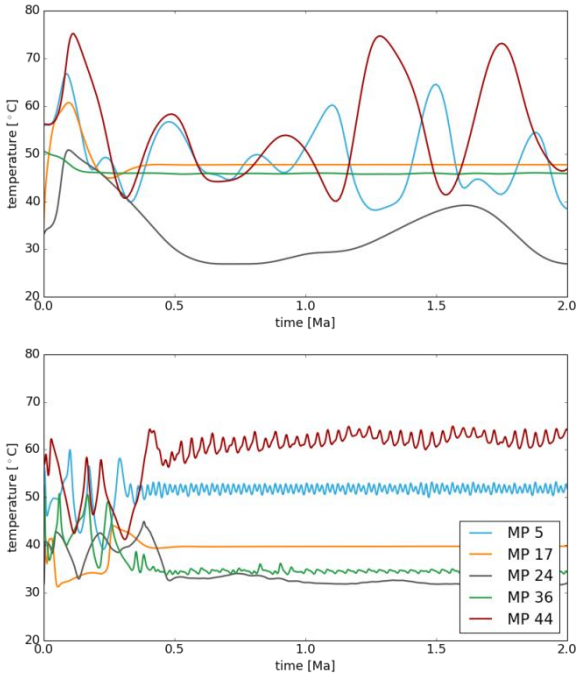

Figure 4: <u>Top:</u> Plot showing temperature history at three monitoring points in the homogeneous scenario. <u>Bottom:</u> Temperature histories at the same three monitoring points in the compaction scenario.

The points in the plots in figure 5 represent at each time step the specific enthalpy in [kJ kg^{-1}] and its change relative to the previous time step. During onset of convection, both scenarios show drastic jumps across the phase space. With propagating time, enthalpies approach a point in phase space, where the change in enthalpy is zero, i.e. $(\partial H/\partial t) = 0$. In the homogeneous scenario, the model orbits a basin of attraction at specific enthalpies between 185 kJ kg^{-1} and 195 kJ kg^{-1}. In the compaction scenario, a cluster is formed in an interval of 180 kJ kg^{-1} and 185 kJ kg^{-1}. However, no clear orbits can be distinguished in the compaction scenario. This may be related to the strongly irregular small-scale oscillations at different monitoring points (see Fig. 4 bottom). Further, the number of time steps in the compaction model is about 8 times higher than in the homogeneous scenario.

Hence, the time between the time steps is smaller, arguing for a more complicated model.

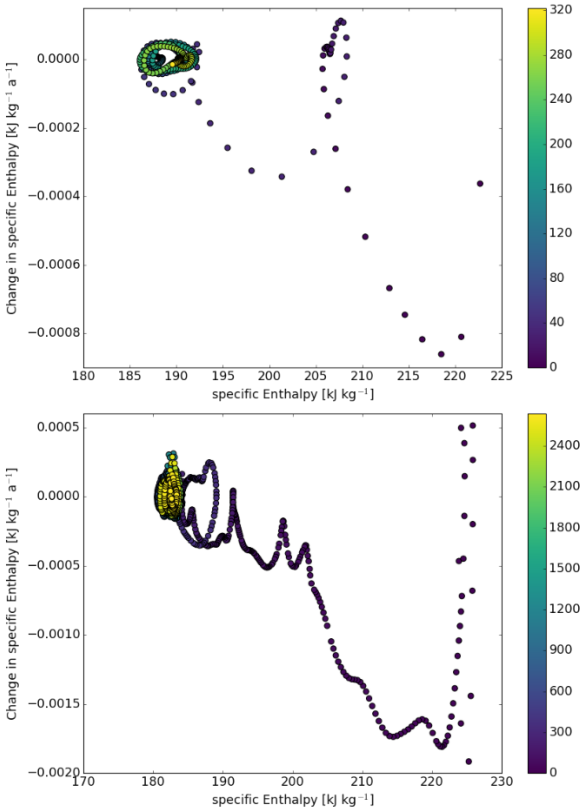

Figure 5: <u>Top:</u> Global attractor of the homogeneous scenario. <u>Bottom:</u> Global attractor of the compaction scenario. Colorscale is indicating time steps.

The convergence towards a certain interval in this phase space suggests that the models reach a representative, dynamic steady state. According to the colored time steps, the homogeneous model approaches an orbit after about 60 time steps, while the compaction model after about 400 time steps.

5.2 Entropy production

We now evaluate the entropy production within our model scenarios in order to assess whether a heterogeneous permeability distribution has a significant impact on the magnitude of entropy production compared to a homogeneous permeability in the reservoir. Before describing and comparing the calculated entropy productions for each scenario, the connection between convection and entropy production is explained.

Figure 6 shows a cross-section through our 3D model (heterogeneous scenario). Within the Yarragadee Aquifer (Fig. 6 top), free convection occurs (Fig. 6 middle). The corresponding entropy production (Fig. 6 bottom) shows that entropy is primarily produced between zones of upflow and zones of downflow in the convecting layer, so in-between convective rolls. We plot entropy production as $\sqrt[3]{dS/dt}$ for better visualisation (Wellmann, 2013)

All our models show Rayleigh numbers far bigger than the critical. In such cases, an average value of entropy production may not be distinctive for a particular cellular mode of the convective layer, i.e. the number of upwelling and downwelling zones in the reservoir. It acts more as an indirect indicator for the complexity and uncertainty of the system. However, it may serve as an indicator for the magnitude of uncertainty of the uniqueness of the convective system (Börsing et al., 2016).

Figure 7 shows a representative plot of entropy production in our model scenarios. In this presentation, the heterogeneous scenario has the highest absolute values of entropy production, and the influence of heterogeneous permeability on the geometry of the convective system is clearly visible.

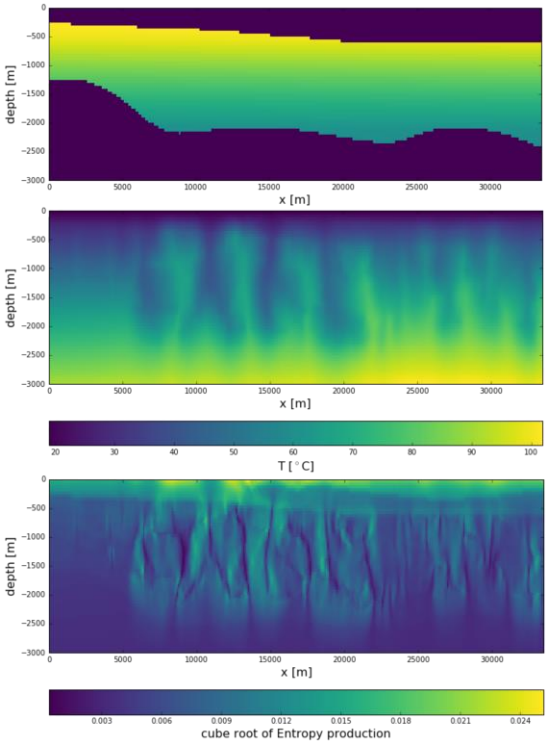

Figure 6: E-W Cross section through the model. <u>Top:</u> Geometry of the Yarragadee Aquifer. <u>Middle:</u> Temperature Field showing free convection. <u>Bottom:</u> Corresponding cube root of entropy production of the convecting layer.

The homogeneous scenario shows higher entropy production between zones of upflow and zones of downflow (narrow dark lines). High entropy production is observed in the eastern part of the model near the darling fault. At this location, higher values of entropy production are also observed in the compaction scenario. This may be related to strong, localised convection in this area. Overall, entropy production in the compaction scenario seems to be lower compared to the other scenarios. Due to the reduced thickness of a highly permeable aquifer in the compaction scenario, convection cells are much narrower, which is mimicked by the entropy production.

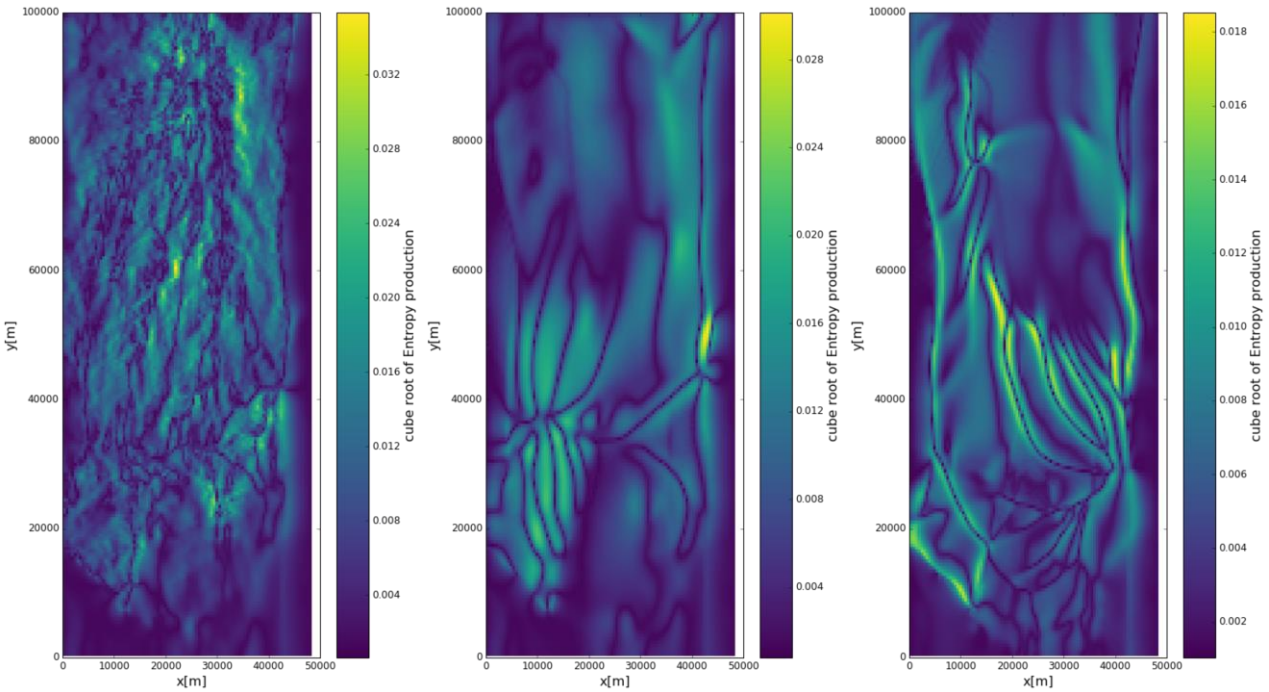

Figure 7: Cube root of entropy production at 2 km depth for all three model scenarios. A) with heterogeneous permeability, B) with homogeneous permeability, C) compaction scenario.

However, contrary to the observations in Figure 7, the compaction scenario exhibits the highest average entropy production of all three scenarios (Fig. 8). Considering the mean entropy production, the homogeneous and heterogeneous scenarios differ only by around $1.02e^{-7}$ W m^{-3} K^{-1}, whereas the average entropy production of the compaction scenario is approximately a factor 1000 higher.

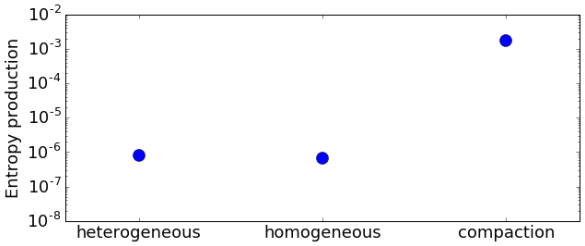

Figure 8: Average entropy production of the three scenarios.

These findings suggest that a heterogeneous permeability distribution does not have a significant influence on the entropy production in our model compared to a homogeneous scenario. Thus, the reservoir geometry, i.e. its lateral extent vs. its vertical extent, seem to control the convection mode, and therefore the entropy production in the reservoir system. However, a decrease in permeability with depth seems to have a big influence. This may be explained by an increased number of convection cells, hence an increased lateral heat flow.

3. CONCLUSIONS

Our hydrothermal models of the Central Perth Basin are characterised by free convection in the Yarragadee Aquifer. Oscillating convection cells introduce higher complexity into the numerical model, and no real steady state is reached. In this study, we therefore used a phase space representation of our models in order to assess whether a dynamic steady state is reached after a certain time. In the evaluated scenarios, all models reach a dynamic steady state. That is, their solution orbits around a point or an interval in phase space. It should be noted that we used attractors as a measure to better evaluate and understand if, and when, our system reaches a dynamic steady state. This analysis has implications for optimising the computational cost, as simulations may be terminated once their solution is in a stable orbit in phase space. The value of representing a model solution in phase space is debatable. However, our simulations suggest that it may serve as an ancillary tool for assessing model (convergence) behaviour.

We furthermore used the measure of entropy production as a representative measure for evaluating the convective pattern in the different scenarios. Our findings suggest that heterogeneous permeability has a subordinate influence on the magnitude of entropy production in the model. This finding is supported with results from synthetic model assessments (Börsing et al., 2016). Due to the irregular geometry of the Yarragadee Aquifer, entropy production is not really useful to predict a preferred cellular mode of the convective pattern, as these modes are usually connected to specific aspect ratios, i.e. ratios of lateral- vs vertical extent of the reservoir.

The compaction scenario showed the highest average entropy production compared to the other scenarios. This is an example of entropy production indicating an increased uncertainty of the modelled convective pattern. The strongly irregular oscillation in many

monitoring points also supports a higher uncertainty connected to the modelled convective system (Fig. 4 and Fig. 5). It may be concluded that the convective pattern shown of our compaction scenario (Fig. 7 c) is the most uncertain of the three scenarios. This suggests that reservoir structure, i.e. effective thickness of the convecting layer has a stronger influence on the convective pattern than spatially heterogeneous permeability.

REFERENCES

Awrejcewicz, J: Classical mechanics: Dynamics. Vol. 29. *Springer Science & Business Media*, NewYork, (2012).

Börsing, N.: Entropy Production in Convective Hydrothermal Systems. *Unpublished Master's thesis, RWTH Aachen University*, (2015).

Börsing, N., Wellmann, F., Niederau, J.: Entropy production in convective hydrothermal systems. *Poster, presented at 2016 EGU General Assembly*, Vienna, Austria, 17 – 22 Apr, (2016).

Costa, V. A. F. "On natural convection in enclosures filled with fluid-saturated porous media including viscous dissipation." *International journal of heat and mass transfer* 49.13, 2215-2226, (2006).

Corbel, S., Schilling, O., Horowitz, F. G., Reid, L. B., Sheldon, H. A., Timms, N. E., and Wilkes, P.: Identification and geothermal influence of faults in the Perth Metropolitan Area, Australia. In *Thirty-Seventh Workshop on Geothermal Reservoir Engineering, Stanford, CA*, (2012).

Crostella, A. & Backhouse, J.: Geology and petroleum exploration of the central and southern Perth Basin, Western Australia, Vol. 57, *Geological Survey of Western Australia*, (2000).

Enns, R. H., and McGuire, G. C.: Nonlinear Physics with Mathematica for Scientists and Engineers, *Birkhäuser Boston*, (2001).

Kern, R. and Weisbrod, A.: Thermodynamics for geologists. *Freeman, Cooper Co.*, (1967).

Niederau, J.: Calibration of a Fractal Model Relating Porosity to Permeability and its Use for Modeling Hydrothermal Transport Processes in the Perth Basin, Australia. *Energy Procedia*, *59*, 293-300, (2014).

Niederau, J., Ebigbo, A., Freitag, S., Marquart, G., Hentschel, B., and Clauser, C.: On the Impact of Spatial Permeability Heterogeneity on the Characteristic Wavelength of Free Convection Cells in the Perth Basin, Australia. *Proceedings World Geothermal Congress, Melbourne, Australia*, (2015).

Nield, D. A., and Adrian B.: Convection in porous media. *Springer Science & Business Media*, New York (1999).

Pujol, M., Ricard, L. P., & Bolton, G.: 20 years of exploitation of the yarragadee aquifer in the perth basin of western australia for direct-use of geothermal heat. *Geothermics*, 57, 39 – 55, (2015)

Playford, P. E., Cockbain, A. E., & Low, G.: Geology of the Perth Basin, Western Australia, *Geological Survey of Western Australia Perth*, (1976).

Reid, L. B., Corbel, S., Poulet, T., Ricar, L.P., Schilling, O., Sheldon, H.A. and Wellmann, J.F.: Project 3: Hydrothermal modelling in the Perth Basin, Western Australia. *WA Geothermal Centre of Excellence*, p. 177, (2012b)

Schilling, O., Sheldon, H. A., Reid, L. B., and Corbel, S.: Hydrothermal models of the Perth metropolitan area, Western Australia: implications for geothermal energy. *Hydrogeology Journal*, *21*(3), 605-621, (2013).

Sheldon, H. A., Florio, B., Trefry, M. G., Reid, L. B., Ricard, L. P., and Ghori, K. A. R.: The potential for convection and implications for geothermal energy in the Perth Basin, Western Australia. *Hydrogeology Journal*, *20*(7), 1251-1268, (2012).

Taylor, R.: Attractors: Nonstrange to Chaotic. *Society for Industrial and Applied Mathematics, Undergraduate Research Online*, (2010), 72-80.

Timms, N. E., Corbel, S., Olierook, H., Wilkes, P., Delle Piane, C., Sheldon, H., Alix,r., Horowitz, F., Wilson, M., Evans, K. A., Griffiths, C., Stütenbecker, L., Israni, S., Hamilton, P.J., Esteban, L., Cope, P., Evans, C., Pimienta, L., Dyt, C., Huang, X., Hopkins, J. and Champion, D.: Project 2: Geomodel. *WA Geothermal Centre of Excellence*, p. 188, (2012).

Wagner, W., et al.: The IAPWS industrial formulation 1997 for the thermodynamic properties of water and steam. *Journal of Engineering for Gas Turbines and Power* 122.1: 150-184, (2000).

Wellmann, J. Florian: Uncertainties have a meaning *(PhD Thesis). (K. Regenauer-Lieb, Ed.). University of Western Australia*, Perth, (2013).